

International Journal of Polymeric Materials and Polymeric Biomaterials

Publication details, including instructions for authors and subscription information:

<http://www.tandfonline.com/loi/gpom20>

Characterization of PLGA/Chitosan Electrospun Nano-Biocomposite Fabricated by Two Different Methods

Sedigheh Vaezifar ^{a b}, Shahnaz Razavi ^a, Mohammad Ali Golozar ^b, Hamid Zarkesh Esfahani ^c, Mohammad Morshed ^d & Saeed Karbasi ^e

^a Department of Anatomical Sciences and Molecular Biology, School of Medicine , Isfahan University of Medical Sciences , Isfahan , Iran

^b Department of Materials Engineering , Isfahan University of Technology , Isfahan , Iran

^c Department of Biology , Isfahan University of Medical Sciences , Isfahan , Iran

^d Department of Textile Engineering , Isfahan University of Technology , Isfahan , Iran

^e Department of Medical Physics and Biomedical Engineering, School of Medicine , Isfahan University of Medical Sciences , Isfahan , Iran

Published online: 16 Oct 2014.



[Click for updates](#)

To cite this article: Sedigheh Vaezifar , Shahnaz Razavi , Mohammad Ali Golozar , Hamid Zarkesh Esfahani , Mohammad Morshed & Saeed Karbasi (2015) Characterization of PLGA/Chitosan Electrospun Nano-Biocomposite Fabricated by Two Different Methods, International Journal of Polymeric Materials and Polymeric Biomaterials, 64:2, 64-75, DOI: [10.1080/00914037.2014.886244](https://doi.org/10.1080/00914037.2014.886244)

To link to this article: <http://dx.doi.org/10.1080/00914037.2014.886244>

PLEASE SCROLL DOWN FOR ARTICLE

Taylor & Francis makes every effort to ensure the accuracy of all the information (the "Content") contained in the publications on our platform. However, Taylor & Francis, our agents, and our licensors make no representations or warranties whatsoever as to the accuracy, completeness, or suitability for any purpose of the Content. Any opinions and views expressed in this publication are the opinions and views of the authors, and are not the views of or endorsed by Taylor & Francis. The accuracy of the Content should not be relied upon and should be independently verified with primary sources of information. Taylor and Francis shall not be liable for any losses, actions, claims, proceedings, demands, costs, expenses, damages, and other liabilities whatsoever or howsoever caused arising directly or indirectly in connection with, in relation to or arising out of the use of the Content.

This article may be used for research, teaching, and private study purposes. Any substantial or systematic reproduction, redistribution, reselling, loan, sub-licensing, systematic supply, or distribution in any form to anyone is expressly forbidden. Terms & Conditions of access and use can be found at <http://www.tandfonline.com/page/terms-and-conditions>

Characterization of PLGA/Chitosan Electrospun Nano-Biocomposite Fabricated by Two Different Methods

SEDIGHEH VAEZIFAR^{1,2}, SHAHNAZ RAZAVI¹, MOHAMMAD ALI GOLOZAR², HAMID ZARKESH ESFAHANI³, MOHAMMAD MORSHED⁴, and SAEED KARBASI⁵

¹Department of Anatomical Sciences and Molecular Biology, School of Medicine, Isfahan University of Medical Sciences, Isfahan, Iran

²Department of Materials Engineering, Isfahan University of Technology, Isfahan, Iran

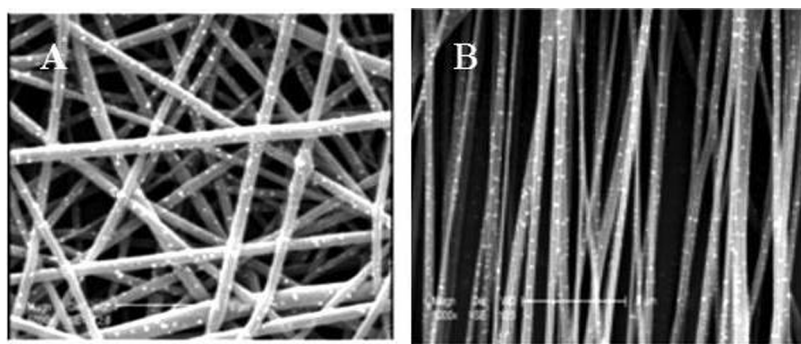
³Department of Biology, Isfahan University of Medical Sciences, Isfahan, Iran

⁴Department of Textile Engineering, Isfahan University of Technology, Isfahan, Iran

⁵Department of Medical Physics and Biomedical Engineering, School of Medicine, Isfahan University of Medical Sciences, Isfahan, Iran

Received 2 November 2013, Accepted 19 January 2014

Nano-biocomposites composed of poly (lactide-co-glycolide) (PLGA) and chitosan (CS) were electrospun using two fabrication methods. In the single nozzle method, the CS nano-powders dispersed in PLGA solutions were electrospun through a single nozzle but in the double-nozzle method, PLGA and CS were simultaneously electrospun from two syringes and the electrospun PLGA nanofiber and electrosprayed CS nanoparticles were mixed and collected on the rotating drum (randomly oriented [A] and aligned [B]) to prepare the nano-biocomposite membrane. The PLGA/CS scaffolds were prepared at the different ratios. The single-nozzle method was associated with decreasing fiber diameter when the CS content was increased and exhibited improve mechanical and hydrophilic properties.



Keywords: Chitosan nanoparticles, electrospinning, nano-biocomposite, PLGA

1. Introduction

Many researchers have employed the electrospinning technique to fabricate biodegradable and biocompatible scaffolds [1–5]. Biodegradable and biocompatible synthetic or natural polymers have been used to develop scaffolds especially designed to mimic the structure and biological

function of the native extracellular matrix (ECM) proteins. Such scaffolds provide the mechanical support required and enhance the cell attachment and proliferation rate [6]. Among the current methods used for fabricating tissue engineering scaffolds, electrospinning has many advantages. It is a simple and convenient technique for producing fine fibers with diameters ranging from nanometer to micron scales. The polymeric scaffolds fabricated by electrospinning are promising materials or substrates [7–9] with high specific surface area, high porosity, and interconnected pores similar to the natural extracellular matrix (ECM), which can regulate cell activities [10]. Both synthetic polymers and natural materials, though different in nature, have been used for fabricating biomedical scaffolds [11,12]. Some of the natural

Address correspondence to: Shahnaz Razavi, Department of Anatomical Sciences and Molecular Biology, School of Medicine, Isfahan University of Medical Sciences, Isfahan, 81744–176, Iran. E-mail: razavi@med.mui.ac.ir

Color versions of one or more of the figures in the article can be found online at www.tandfonline.com/gpom.

and synthetic polymers more commonly used as tissue engineering scaffolds for different tissue reconstruction applications include poly caprolactone (PCL) [13,14], poly(lactide-co-glycolide) (PLGA) [15–17], poly(L-lactide acid) (PLLA) [18–20], poly(3-hydroxybutyrate-co-3-hydroxyhexanoate) (PHBHHx) [21], poly(3-hydroxybutyrate-co-3-hydroxyvalerate) (PHBV) [22], gelatin [23,24], collagen [25,26], and chitosan [27,28]. PLGA, as a synthetic polymer, has been used for both soft and hard tissue regeneration and its long history of successful applications has attracted attention for use as a biomaterial [29]. Based on studies over the past few decades, PLGA degrades via chemical hydrolysis of the hydrolytically unstable ester bond into the non-toxic and biocompatible lactic and glycolic acids. PLGA's degradation rate is affected by its molecular weight (MW), copolymer composition, crystallinity, and other structural characteristics [29]. Mechanical flexibility, low antigenicity, ease of processing, and low degrees of chronic persistence are among its advantages. Hydrolysis of PLGA produces nonpolymeric lactic and glycolic acids that can be metabolized into water and carbon dioxide via the tricarboxylic acid cycle [30,31]. Moreover, the mechanical properties of PLGA make it especially useful as a biomedical scaffold in tissue engineering [32]. However, its disadvantages include high hydrophobicity, low water absorptivity, low cell attachment, and low cell proliferation rate [33]. To overcome these shortcomings, materials composed of both synthetic and natural polymers have been proposed that are very similar to macromolecular substances and that can be detected and metabolized in a biological environment [34–36]. Chitosan is an excellent example of natural, nontoxic biopolymers due to its biological properties such as biodegradability, biocompatibility, antibacterial effect, and wound-healing activity, all of which make it one of the most promising biopolymers for use in tissue engineered scaffolds [37–39]. It is commercially produced by the partial deacetylation of chitin, which is obtained from the exoskeleton of crustaceans and the cell wall of fungi. Chitosan has found numerous applications as a polycationic and nontoxic polymer in food, pharmaceutical, and chemical industries [40]. Its positively charged surface offers favorable conditions for the improved adhesion and growth of different types of cells [41–45]. Finally, nontoxic monosaccharides and oligosaccharides are produced via enzyme-degradation of chitosan [46].

Fabrication of nanofibers from pure chitosan is limited by the high repulsive forces between the ionic groups within the polymer backbone arising due to the application of a high electric field during electrospinning [47]. An alternative strategy involves the fabrication of composite materials by compositing or electrospinning of blend solutions. In this strategy, the typical materials for compositing or blending with chitosan are poly(vinyl alcohol) (PVA) [48], poly(ethylene oxide) (PEO) [49], poly(ethylene terephthalate) (PET) [50], and poly(lactic acid) (PLA) [51]. Compared to pure chitosan, these composites enjoy such advantages as higher mechanical strength, biocompatibility, and antibacterial properties [52]. Hong and Kim [53] described two processing methods for the fabrication of PCL/chitosan biocomposites. In one case, chitosan was used to reinforce electrospun PCL nanofibers by electrospinning a mixture of PCL solution and

chitosan powders in a single step. In the other case, chitosan was deposited on electrospun PCL fibers by air-spraying.

The current study describes two processing methods, reported here for the first time, for the fabrication of PLGA/CS biocomposites. The first method, named the single-nozzle electrospinning, involves electrospinning a mixture of PLGA solution and chitosan nano-powders through a single nozzle. The second, named the double-nozzle electrospinning, describes the deposition of chitosan nanoparticles on electrospun PLGA nanofibers by electrospraying the chitosan solution. The chitosan nano-powder used in the first method was prepared by the ionic gelation method reported in our previous work [54]. Because of high hydrophobicity, and low cell attachment of PLGA, chitosan nanoparticles were used to overcome these shortcomings, in this study. The mechanical properties of PLGA make it especially useful as a biomedical scaffold in tissue engineering. Scaffold composed of PLGA and chitosan nanoparticles provide the mechanical support required and enhance the cell attachment and proliferation rate. In the current study, chitosan nanoparticles and PLGA were used to fabricate the scaffolds by electrospinning method, for the first time. Randomly oriented and aligned PLGA and PLGA/CS biocomposite nanofibrous matrices (with the different PLGA/CS ratios of 90/10%, 80/20%, and 70/30% w/w) were successfully prepared via both methods. The scaffolds thus produced were subsequently characterized in terms of their physicochemical properties, water contact angles, swelling, mechanical properties, morphology, and biodegradation behavior.

2. Experimental

2.1 Materials

PLGA (LA/GA 85/15; Mw = 50,000–75,000) and acid-soluble chitosan (low molecular weight with a deacetylation degree of >85%) were purchased from Sigma-Aldrich (St. Louis, MO, USA). The two solvents 2, 2, 2-trifluoroethanol (TFE) and trifluoroacetic acid (TFA) were selected for PLGA and chitosan, respectively, both purchased from Merck (Darmstadt, Germany). All other reagents were purchased from Merck.

2.2 Fabrication of Scaffolds

2.2.1 Fabrication of Pure Electrospun PLGA Nanofiber

Commercially available PLGA granules were dissolved in TFE. The block PLGA copolymer solution was loaded in a 1 mL syringe. An electric field (a high-voltage DC power supply of 0–45 kV) was created between the needle used as the anode and the collecting drum used as the cathode. The polymer solution was drawn from the syringe under an accurate infusion control pump (JMS SP 500, Japan). Randomly oriented PLGA nanofibers and aligned ones were collected on a rotating drum (50 mm in diameter) and wrapped with aluminum foil at 50 rpm and 4000 rpm, respectively. All the experiments were carried out at room

temperature. The scaffolds were dried overnight under vacuum at room temperature. To obtain the optimum conditions for the fabrication of electrospun nanofibers, the effects of such parameters as polymer solution concentration, feed rate, voltage, and distance of collector from the needle tip were investigated on the morphology and diameter distribution of electrospun nanofibers.

The optimum conditions were obtained with a polymer solution concentration of 24% w/v at a feeding rate of 0.25 mL/h and a high voltage of 13.5 kV. The distance of collector from the needle tip was 10 cm.

2.2.2 Nano-Biocomposite Preparation by Electrospinning of PLGA/Chitosan

The PLGA/CS nano-biocomposites were electrospun onto a rotating collector from a PLGA solution (24% w/v in TFE) containing different weight ratios of 10, 20, and 30 wt% chitosan nano-powders prepared by the ionic gelation method as described in our previous work [54]. The homogenous solutions were obtained by slowly adding chitosan nano-powders and gentle stirring for 12 h at room temperature. The same optimum electrospinning conditions were obtained as mentioned previously.

For the double-nozzle method, the deposition of chitosan nanoparticles on the electrospun PLGA fibers was initially optimized by electro-spraying the chitosan solution into nano-sized particles at a lower concentration with negligible chain entanglement. This is because continuous fibers cannot be produced by electrospinning at high concentrations. Chitosan nanoparticles were distributed uniformly on the PLGA nanofibrous structure by simultaneous electrospinning, and the nanoparticles appeared to adhere strongly to the PLGA nanofibers. In this method, chitosan was dissolved in TFA at a concentration of 2% w/v before being sprayed onto the target by electrostatic charge and at a feeding rate of 0.33 mL/h and an applied voltage of 13–14 kV. The distance between the spraying nozzle and the mat was 10 cm. In the double-nozzle method, the PLGA and chitosan solutions were simultaneously electrospun from two different syringes and mixed on the rotating drum to prepare the nanofibrous biocomposite membrane. A 90/10 weight ratio of PLGA/CS was obtained by simultaneous electrospinning of the two solutions. To obtain the 80/20 and 70/30 weight ratios of PLGA/CS, the duration of electro-spraying the chitosan solution was increased without electrospinning the PLGA solution in multi-steps. Randomly oriented PLGA/CS nano-biocomposites and aligned nanofibers were formed using a rotating drum at 50 and 4000 rpm, respectively. The fabricated scaffolds were dried overnight under vacuum at room temperature.

2.3 Characterization of Scaffolds

2.3.1 Morphology

Electrospun nanofibrous membranes were sputtered with gold, and their morphology was observed using a scanning electron microscope (SEM; Seron Technology AIS 2500, India). The diameters of the resulting nanofibers were determined using the Image J software from the SEM

micrographs. The sample thickness was evaluated using cross sections prepared by cryocut (cryocut 1800, reichert, JUNG, Germany) and measured by the Image J software at three points. The measured values were averaged. A Philips CM12 transmission electron microscope, operated at 120 kV was used to investigate the distribution of nanoparticles. TEM micrographs showed a good distribution of chitosan nanoparticles in the PLGA fiber prepared by the single-nozzle method.

2.3.2 Water Contact Angle (WCA)

To evaluate the effect of chitosan on the hydrophilicity of electrospun PLGA fiber webs, WCAs were measured using a contact angle analyzer (Dataphysics, Model: OCA 15 plus, Canada). Measurements were acquired at five independent points and presented as the average value \pm standard deviation (SD).

2.3.3 PBS Absorption (Swelling)

Electrospun membranes of PLGA and PLGA/CS were cut into 10 mm \times 10 mm square shapes for PBS absorption. Pre-weighed specimens were placed in closed bottles containing 10 mL of PBS ($\text{pH} = 7.40$) and incubated in vitro at $37.0 \pm 0.1^\circ\text{C}$ for 24 h. The wet weight of the membranes was determined by weighing them immediately on an electronic balance after removing the membranes from PBS and dehydrating them with filter paper to absorb water on the membrane surface. The water uptake of the electrospun membranes in PBS were then calculated using Eq. 1:

$$\text{Swelling}(\%) = (w_1 - w_0/w_0) \times 100\% \quad (1)$$

where, w_0 and w_1 are the weights of the membranes before and after immersion in the PBS, respectively.

2.3.4 Mechanical Properties

The specimens were carefully cut into 10 mm \times 50 mm rectangular strips, and their tensile properties were evaluated using a tensile testing machine (Zwick Tensile Tester, 1446, Germany) equipped with a 20-N load-cell. The cross-head speed was 10 mm/min. The reported tensile moduli, tensile strengths, and elongations were presented as averages of three tests.

2.3.5 Biodegradation Behavior

The loss of scaffold weights was evaluated after cultivation. The biodegradation behavior of the scaffolds was evaluated by measuring the weight change in PBS as follows. The initial mass of the scaffolds was measured. They were then allowed to degrade by placing them in phosphate buffer solution pH 7.4 and incubated at 37°C . At selected time intervals (1, 2, 7, 14, 21, and 30 days), the scaffolds were removed from the solution, blotted with an absorbent tissue, dried in a vacuum oven, and weighed. The biodegradation percentage, D (%), was defined as in Eq. 2:

$$D(\%) = (w_i - w_f/w_i) \times 100\% \quad (2)$$

where w_i is the initial weight of the scaffold and w_f is the final weight of scaffold at the selected time intervals.

Table 1. Characteristics of the nanofibrous scaffold

Average fiber diameter (nm)	Method of composite preparation	Fiber orientation	PLGA/CS	Scaffold nomenclature
486 ± 32	PLGA only	Random	100/0	100 R
423 ± 30	PLGA only	Align	100/0	100 A
393 ± 24	Single-nozzle method	Random	90/10	1090 Rd
364 ± 22	Single-nozzle method	Random	80/20	2080 Rd
320 ± 21	Single-nozzle method	Random	70/30	3070 Rd
352 ± 23	Single-nozzle method	Align	90/10	1090 Ad
309 ± 20	Single-nozzle method	Align	80/20	2080 Ad
286 ± 18	Single-nozzle method	Align	70/30	3070 Ad
435 ± 38	Double-nozzle method	Random	90/10	1090 Re
435 ± 38	Double-nozzle method	Random	80/20	2080 Re
435 ± 38	Double-nozzle method	Random	70/30	3070 Re
376 ± 31	Double-nozzle method	Align	90/10	1090 Ae
376 ± 31	Double-nozzle method	Align	80/20	2080 Ae
376 ± 31	Double-nozzle method	Align	70/30	3070 Ae

R = randomly oriented nanofibrous web; A = align-oriented nanofibrous web; d = dispersing chitosan nano-powders in PLGA solution; e = electro-spraying the chitosan solution on the PLGA nanofibers.

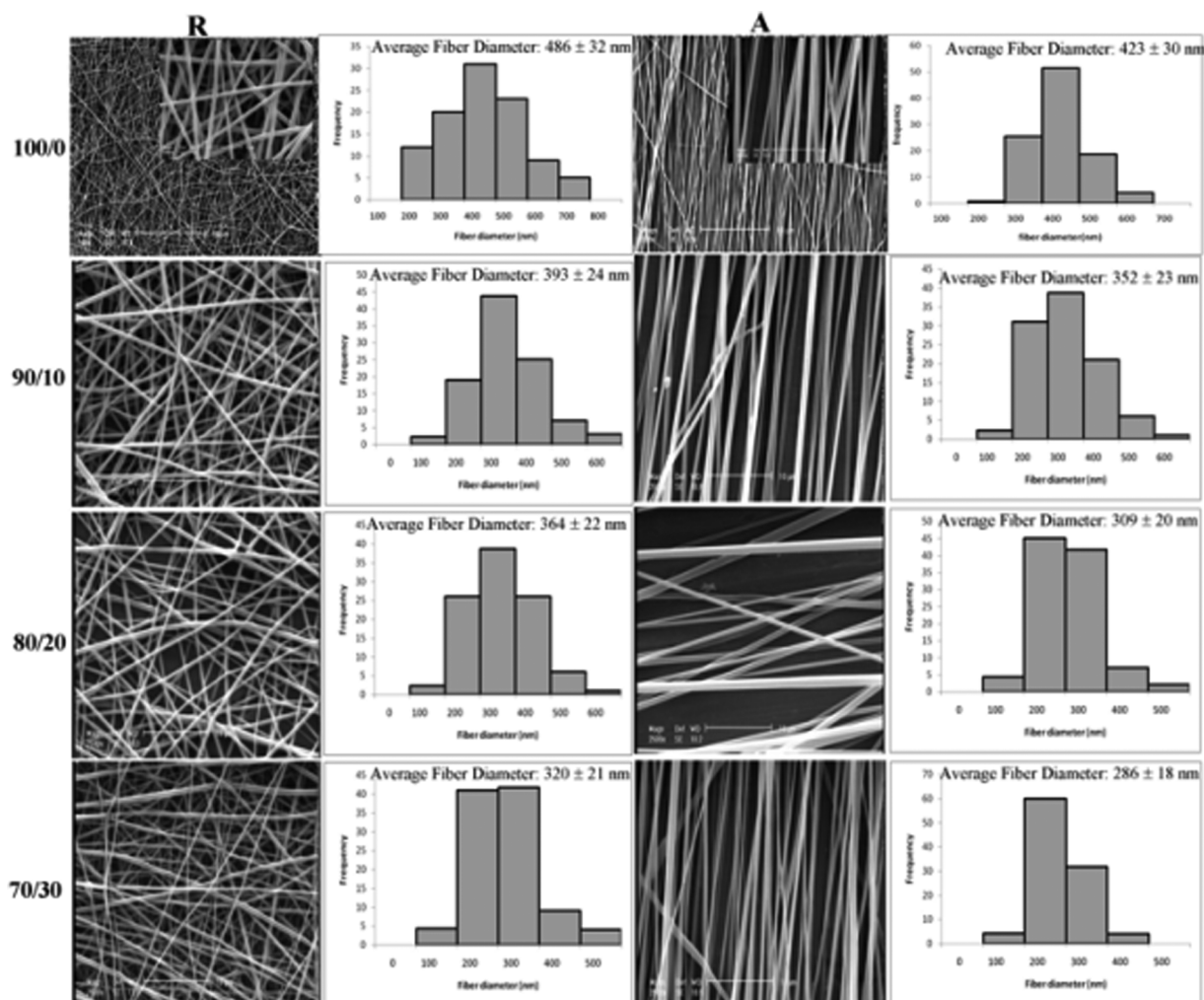


Fig. 1. SEM micrographs and diameter distribution of PLGA and PLGA/CS (90/10%, 80/20%, and 70/30% w/w) electrospun fibers fabricated by single-nozzle method.

2.3.6 Attenuated Total Reflection Fourier Transform Infrared (ATR-FT-IR)

Chemical characteristics of the electrospun PLGA and PLGA/CS nanofibrous scaffolds and pure powders of chitosan were evaluated by an attenuated total reflection Fourier transform infrared (ATR-FT-IR) spectrophotometer (JASCO FT/IR-6300, Japan). All spectra represent the average of 30 scans between 400 and 4000 cm⁻¹.

2.3.7 Thermal Property

The thermal property of the scaffolds was studied using the thermogravimeter (TG, Rheometric Scientific, Inc 1998, USA) at a constant heating rate of 10°C/min over a temperature range of 25–600°C.

2.4 Statistical Analysis

All the data in this paper were presented as means \pm standard deviation and analyzed using single-factor analyses of variance (ANOVAs). The significance level was set at $p < 0.05$.

3. Results

3.1 Morphology of Electrospun Nanofibers

The morphology of the electrospun nanofibers is influenced by various parameters such as applied voltage, solution feed

rate, distance between the capillary and the collector, and especially the properties of the polymer solutions including concentration, surface tension, and the nature of the solvent [6,55]. The scaffold nomenclature, fiber orientation, method of composite preparation, PLGA/CS ratio and the average fiber diameter (nm) are presented in Table 1. No significant differences ($p < 0.05$) in the diameter were observed for random compared to aligned nanofibers for the respective PLGA and PLGA/CS nanofibers.

Figure 1 shows the morphology of the randomly oriented and aligned electrospun PLGA from a 24% PLGA solution in TFE as the solvent. The insets display the corresponding diameter distribution. As can be seen, highly uniform and smooth nanofibers were formed without the occurrence of bead defects in all the randomly oriented and aligned nanofibrous scaffolds. Using the Image J software of the SEM micrographs, the average fiber diameters of the randomly oriented and aligned PLGA fibers were determined to be 486 ± 32 nm and 423 ± 30 , respectively. Figure 1 also shows the SEM micrograph and the insets display the corresponding diameter distribution of the PLGA/CS electrospun fibers with three different ratios (90/10%, 80/20%, and 70/30% w/w), fabricated by the single-nozzle method. In this method, the chitosan nano-powders dispersed in the PLGA solutions were electrospun through a single nozzle. As shown, the average diameter of the PLGA/CS membrane

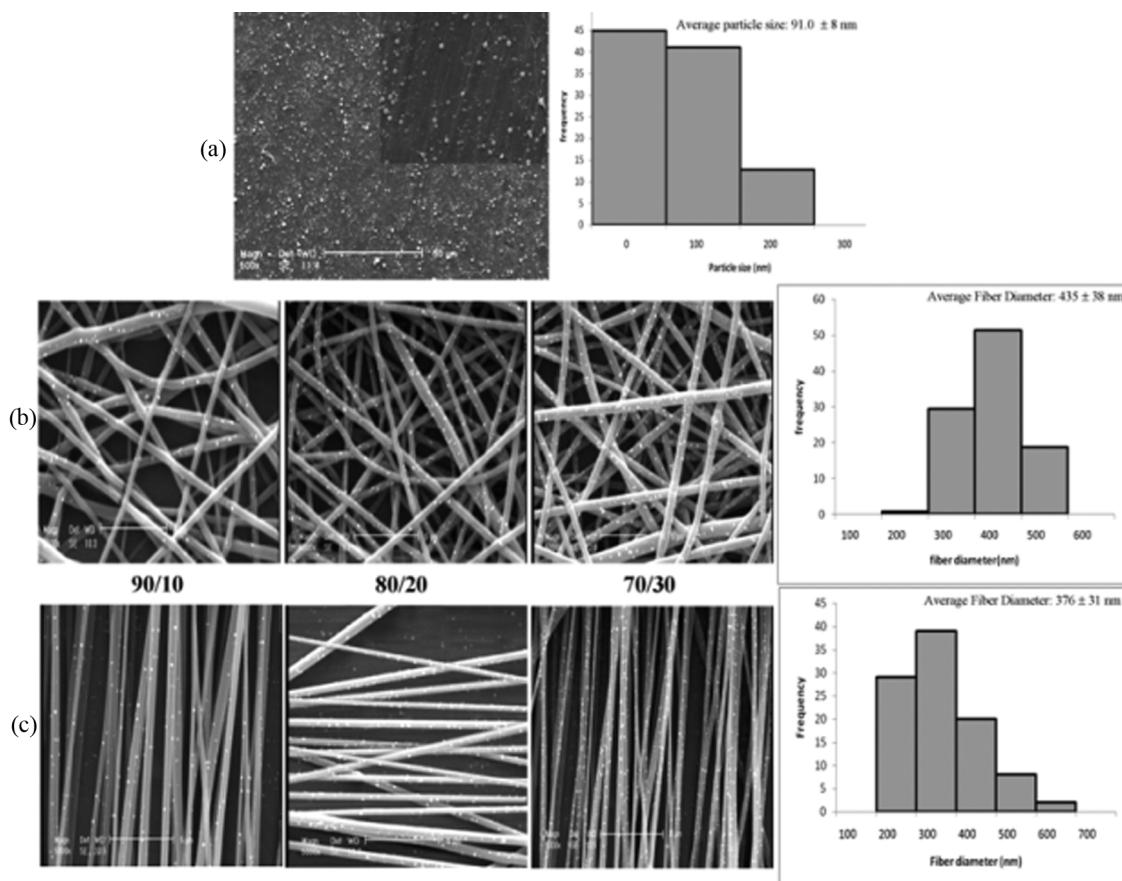


Fig. 2. SEM micrographs and diameter distribution of CS nanoparticles (a), PLGA/CS electrospun fibers in randomly oriented (b), and aligned (c) fibers fabricated by double-nozzle method at three different ratios (90/10%, 80/20%, and 70/30% w/w).

prepared by dispersing the chitosan nano-powders in PLGA solution is lower than the others. The nanofiber diameter decreased and the diameter distribution broadened with increasing chitosan content. There were significant differences ($p < 0.05$) in the diameter by increasing chitosan content. The presence of chitosan in the PLGA solution increased conductivity and surface charge densities, which enhanced the whipping instability.

SEM micrograph of chitosan nanoparticles electro-sprayed from a 2% w/v solution in TFA at a feeding rate of 0.33 mL/h and an applied voltage of 13–14 kV is shown in Figure 2a. The distance between the spraying nozzle and the mat was 10 cm. Chitosan nanoparticles obtained under this condition were highly uniform. However, the average diameter of chitosan particles was 91 ± 8 nm and its distribution was in the range of 26–250 nm. The SEM micrographs and the insets in Figures 2b and 2c display the corresponding diameter distribution of the PLGA/CS electrospun fibers/electro-sprayed nanoparticles with three different ratios (90/10%, 80/20%, and 70/30% w/w) fabricated by the second method. In this method, PLGA and chitosan solutions were simultaneously electrospun from

two different syringes and the electrospun PLGA nanofiber and electro-sprayed CS nanoparticles were mixed and collected on the rotating drum to prepare the nanofibrous composite membrane. As shown, the average fiber diameter of the PLGA/CS electrospun fibers prepared by electro-spraying the chitosan solution on the PLGA nanofibers is lower than the pure PLGA nanofibers but higher than the ones fabricated by the first method. This could be due to the simultaneous effect of two electrical fields. In order to prepare the aligned scaffold, a high speed rotating drum was used as the collector at a speed of 4000 rpm. Compared with the randomly oriented nanofibers, the aligned ones were smaller in diameter but no significant differences ($p < 0.05$) in the diameter were observed.

All the fabricated scaffolds were 70–80 μm in thickness as evaluated by a scanning electron microscope using a cross section prepared by the cryocut at three points and measured by the Image J software. The measured values were reported as averages. Figure 3a shows the SEM micrograph of the sample thickness.

Transmission electron micrographs of the PLGA/CS scaffolds fabricated by the single-nozzle method are shown in

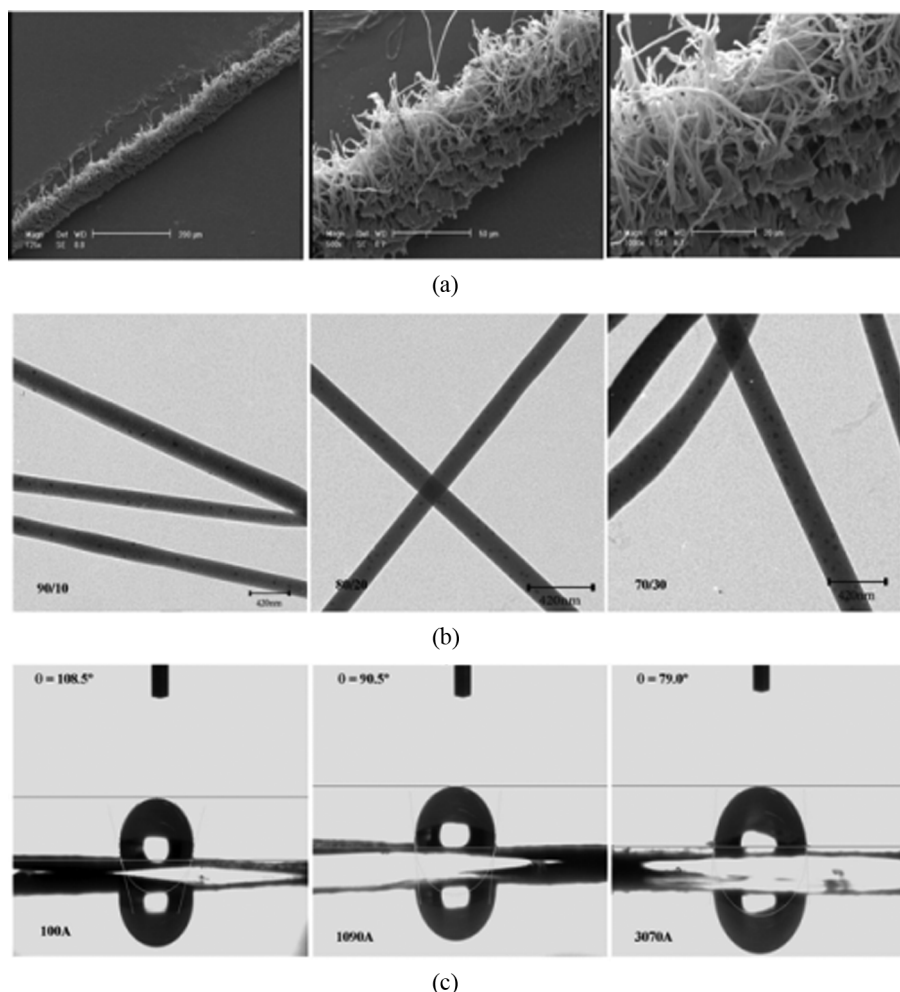


Fig. 3. SEM micrographs of the sample thickness (a), TEM micrographs of PLGA/CS scaffolds fabricated by single-nozzle method (b) and water contact angle of PLGA and PLGA/CS electrospun web (c).

Figure 3b. TEM analysis of the PLGA/CS scaffolds showed that the chitosan nano-powders were well dispersed on the PLGA nanofibers. The distribution indicates that the size of the chitosan nanoparticles on the PLGA/CS scaffolds is smaller than 100 nm. A uniform dispersion of the chitosan nanoparticles on the PLGA nanofibrous was obtained with all the three PLGA/CS ratios (90/10%, 80/20%, 70/30% w/w).

3.2 WCA

To evaluate the effect of chitosan on the hydrophilicity of the composites, WCAs were measured and compared to that of pure PLGA. In general, since chitosan is relatively hydrophilic ($\text{WCA} = 64^\circ$) [56], the biocomposites would likely exhibit a higher hydrophilicity than the pure PLGA web. This hypothesis is confirmed in Figure 3c, where the WCA of a PLGA electrospun mat is higher than that of the 1090 Ad and 3070 Ad. As shown in this figure, the WCA of the PLGA mat is 108.5° . In contrast, the WCAs of 1090 Ad and 3070 Ad decreased to 90.5° and 79° , respectively, when the chitosan content was increased.

3.3 PBS Absorption (Swelling)

Hydrophilicity is important for tissue engineering scaffolds as it enhances cell viability and proliferation rate [57]. The PBS absorption of electrospun scaffolds is shown in Figure 4. As seen, the electrospun net PLGA membrane exhibits the lowest swelling ratio attributed to its hydrophobic nature. It can be seen that the randomly oriented scaffolds have a higher swelling ratio than the aligned ones. Additionally, the results indicated that the PBS absorption of the composite membranes is higher than the electrospun pure PLGA membrane due to the introduction of hydrophilic components (i.e., the chitosan containing hydrophilic hydroxyl and amine groups). Clearly, PBS uptake of the PLGA/CS membrane increased as a result of increased chitosan content in the scaffold. PBS absorption is clearly higher in scaffolds fabricated by the second method than those fabricated by the single-nozzle one due to the high availability of chitosan nanoparticles on the surface of scaffolds prepared by electro-spraying the chitosan solution. Therefore, the PLGA/CS scaffold with a ratio of 70/30 prepared by the second

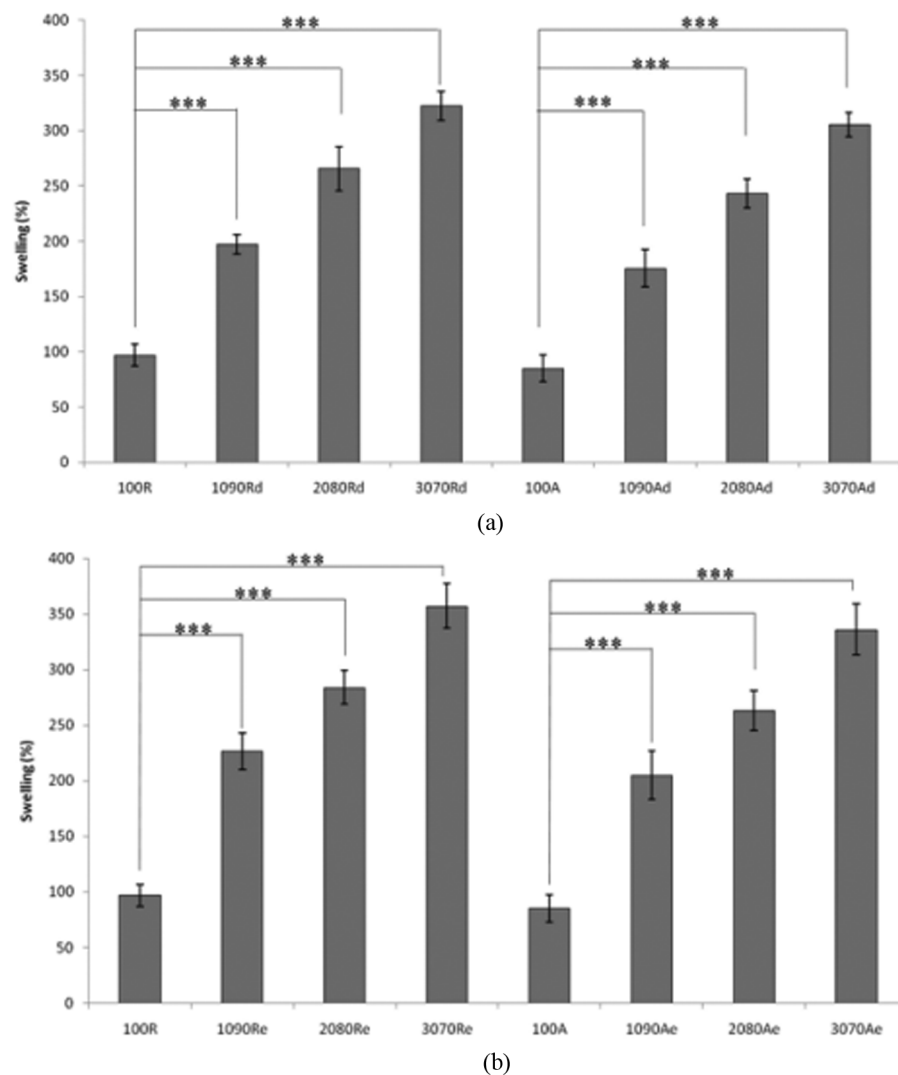


Fig. 4. PBS absorption of electrospun scaffolds fabricated by single-nozzle method (a) and double-nozzle method (**p ≤ 0.001).

method exhibited the highest swelling (Figure 4). It is assumed that the nanofibrous composite membrane of the electrospun PLGA/CS could be potentially used for tissue regeneration.

3.4 Mechanical Properties

Mechanical properties of biomedical substitutes are important in providing physical support for cell growth and migration [58,59]. Figure 5 presents typical stress-strain curves of both randomly oriented and the aligned electrospun PLGA and PLGA/CS nanofibrous scaffolds prepared by the two proposed methods. Clearly, compared with the pure PLGA randomly oriented scaffold, tensile strength (MPa) and Young's modulus (MPa) of the randomly oriented PLGA/CS scaffold increases as the chitosan content is increased. This same trend is observed for the aligned electrospun scaffold as well.

Elongation to break of both randomly oriented and aligned electrospun PLGA/CS nanofibrous scaffolds fabricated by the second method was observed to decrease with increasing chitosan content. However, this was not observed in the case of the PLGA/CS nanofibers fabricated by the single-nozzle method. Thus, it may be concluded that addition of chitosan nano-powders enhanced the mechanical properties of the PLGA/CS composite nanofibrous scaffold produced by the first method because of the reinforcing

effect of nano-powders in the composite. On the contrary, by electro-spraying the chitosan solution in the second method, the electrospun PLGA/CS nanofibrous scaffolds became brittle and their ultimate tensile strain decreased. Additionally, compared with the randomly oriented nanofibrous scaffold, the aligned nanofibrous scaffold exhibited higher tensile strength and Young's modulus, which may be due to the high degree of orientation. In this study, cell culture tests were not performed on the PLGA/CS electrospun scaffolds fabricated by the second method because of the high brittleness.

3.5 Biodegradation Behavior

Figure 6 shows the percentage of weight loss of the PLGA and PLGA/CS scaffolds. It can be seen that the randomly oriented scaffolds have a higher weight loss than their aligned counterparts. Results indicate a faster degradation rate in the composite membranes than in the electrospun pure PLGA ones. Moreover, weight loss increased in the PLGA/CS membrane when chitosan content increased in the scaffolds. As shown in this figure, the rate of weight loss in the PLGA/CS scaffold was faster than that of the chitosan-free one as evidenced by the greater weight loss of about 2.6 times in the 3070 Ad scaffold after 30 days. This is while the rate of biodegradation in the scaffolds fabricated by the second method are faster than those fabricated by the

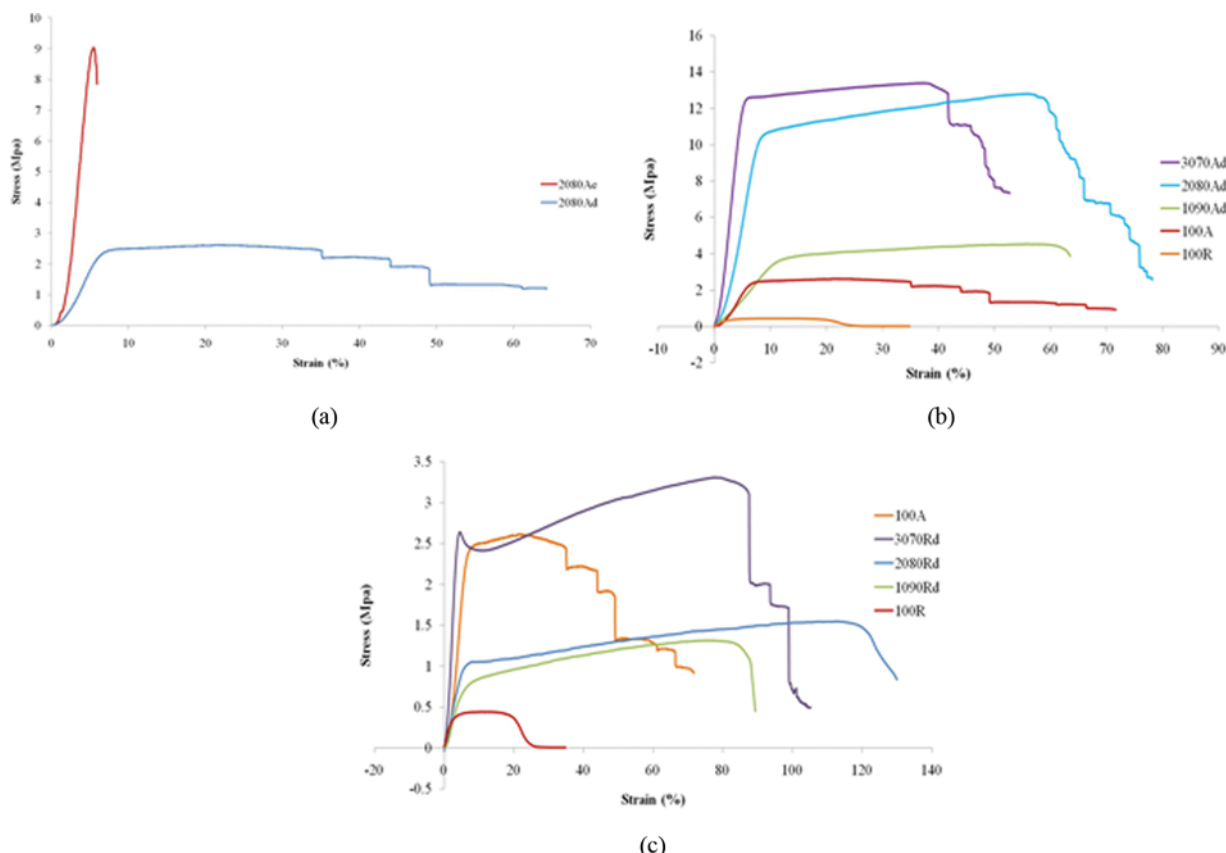


Fig. 5. Stress-strain curves of the PLGA and PLGA/CS nanofibrous scaffolds, comparison of two methods (a), comparison of randomly oriented fibrous scaffolds (b), and comparison of aligned fibrous scaffolds (c).

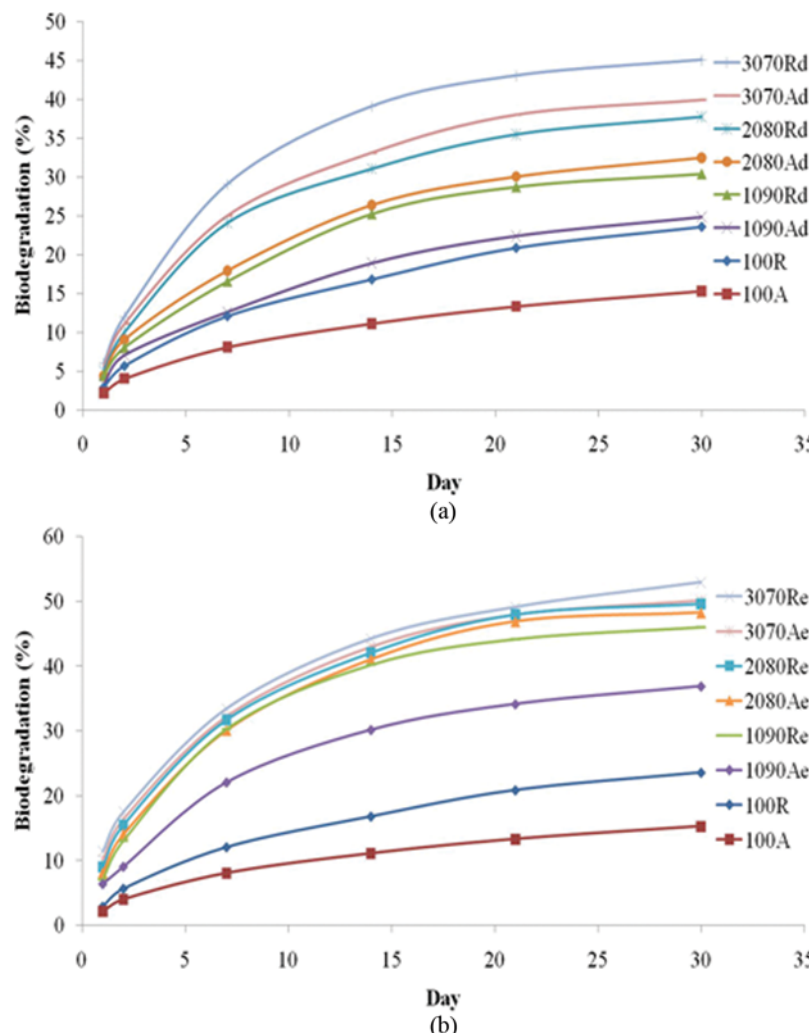


Fig. 6. Biodegradation behavior of the PLGA and PLGA/CS scaffolds fabricated by single-nozzle method (a) and double-nozzle method (b).

first method due to the high availability of chitosan nanoparticles on the surface of the scaffolds prepared by electro-spraying. Figure 6 also shows that weight loss scaffolds increased with time. The main reason for this behavior may be claimed to lie in the hydrolysis of PLGA and enzymatic degradation of hydrophilic chitosan when the scaffolds are maintained in the PBS [29,46].

3.6 ATR-FT-IR

The FT-IR spectra for pure PLGA, pure chitosan, and PLGA/CS composite are shown in Figure 7a. In the case of pure PLGA, the characteristic strong absorption band at about 1752 cm^{-1} is attributed to the stretching vibration of the C–O bond. The bands at 1182 cm^{-1} can be assigned to the C–O–C ether group stretching. The bands at 1130 cm^{-1} and 1452 cm^{-1} are due to the C–O bond and the methyl group C–H bond of the PLGA, respectively [60]. The FTIR spectrum of pure chitosan shows several absorption bands. The absorption bands at 1153 cm^{-1} and 1550 cm^{-1} correspond to the saccharide structure and the

stretching vibrations of C–N coupled to the bending vibrations of N–H in primary amine, respectively. The absorption band at 1655 cm^{-1} corresponds to the stretching vibrations of C–O coupled to the bending vibrations of N–H_{in} acetyl amine. The absorption band at 1717 cm^{-1} corresponds to the stretching vibrations of C–O [46,61,62]. Similar characteristic absorption bands were also observed in the FT-IR spectra of PLGA/CS scaffold. The FTIR spectra of PLGA/CS indicate that chitosan nanoparticles were embedded within the composite scaffold.

3.7 Thermal Property

The TG spectrum is used to determine the weight loss of the material during heating cycle. The thermo gravimetric curve of the pure PLGA, pure chitosan and PLGA/CS scaffolds is shown in Figure 7b. As seen, the decomposition temperature of pure PLGA is about $260\text{--}350^\circ\text{C}$. for the pure chitosan, the initial weight loss at approximately 100°C is due to evaporation of water; while during second range ($350\text{--}450^\circ\text{C}$) corresponds to a complex process including the dehydration

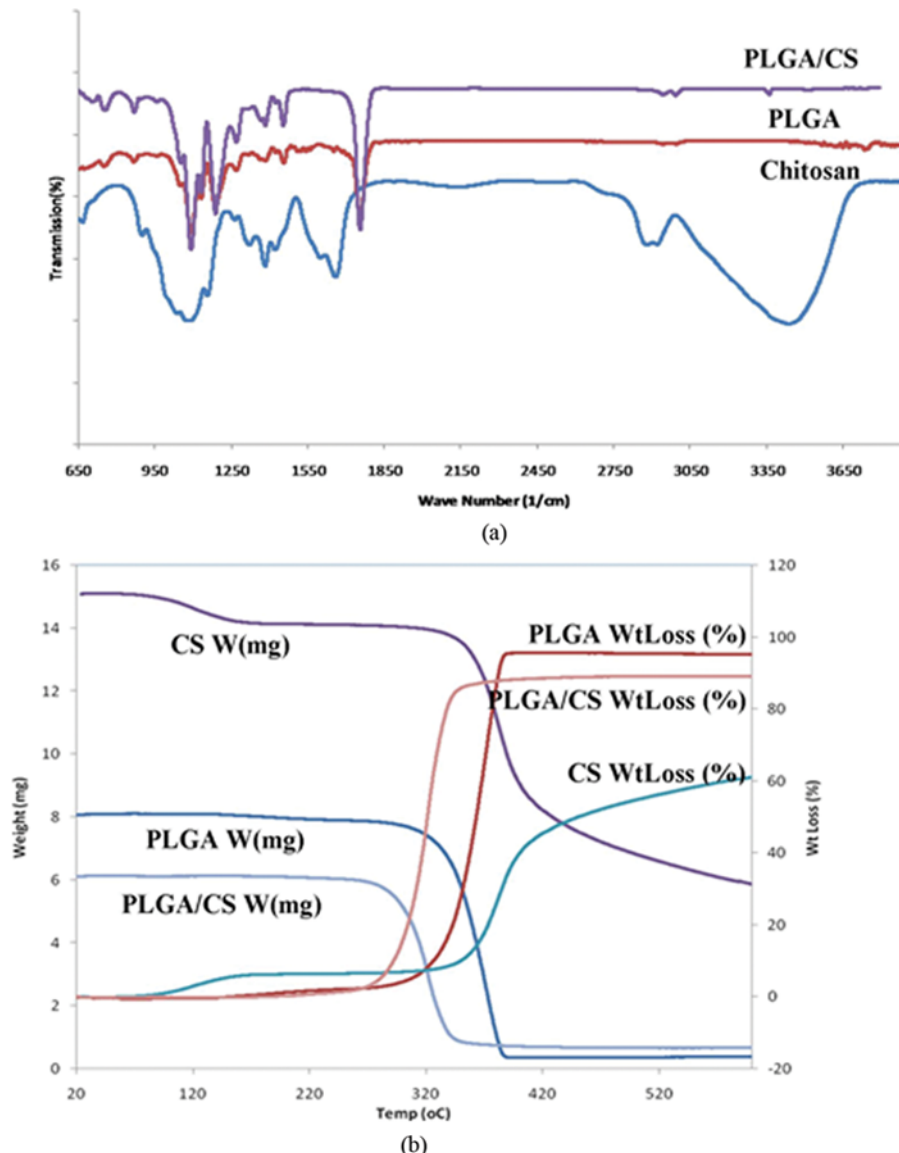


Fig. 7. ATR FT-IR spectrum (a) and TGA curves (b) of the PLGA, chitosan, and PLGA/CS scaffold.

of the saccharide rings, depolymerization, and decomposition of the acetylated and deacetylated units of polymer. The maximum peak observed at 350°C relates to decomposition of sample and indicates the maximum thermal stability of pure chitosan [54,63]. As shown, the hybrid PLGA/CS matrices were thermally decomposed more easily ($250\text{--}320^{\circ}\text{C}$) and they had a lower decomposition temperature, indicating a weaker biomaterial heat resistance.

4. Discussion

In this study, both the randomly oriented and the aligned PLGA and PLGA/CS scaffolds were fabricated using two different, novel methods. Scaffolds were fabricated by dispersing chitosan nano-powders in a PLGA solution in the single nozzle electrospinning method while in the double-nozzle method; the chitosan nanoparticles were electro-sprayed on the PLGA nanofibers. Compared to the

randomly oriented nanofibers, the aligned nanofibers were smaller in diameter due to the drawing effect induced by the rotating drum while the jet contacted the surface of the drum [64]. Chitosan is a kind of natural cationic polyelectrolyte. The presence of chitosan nano-powders in the PLGA solution increased conductivity and surface charge densities, which enhanced the whipping instability [65,66]. In the high electrical field, the PLGA solution containing chitosan nanoparticles underwent a rapid growth of whipping instability and was more elongated to form finer fibers. According to Li et al. [67], the capillary effect of higher porosity can lead to better PBS adsorption. Therefore, it can be seen that the randomly oriented scaffolds have a higher swelling ratio than the aligned ones. Both the WCA and PBS absorption results indicate that the chitosan in the biocomposites give rise to hydrophilicity. This would not only prevent the loss of bodily fluids and nutrients in the in vivo tests, but would also increase the relatively low cell attachment and

proliferation rate of pure PLGA membrane. PLGA containing the hydrophobic methyl group ($-CH_3$) increases the repulsion force when interacting with water and reduces water absorbability. On the contrary, chitosan containing the primary amine ($-NH_2$) and hydroxyl ($-OH$) groups can not only increase its affinity to water but also form hydrogen bonds with water. Hence, more chitosan in the PLGA/CS matrix generally enhances the hydrophilic property of the biomaterial surfaces for water entrapment.

Orientation of the fabricated fibers is one of the important factors in the preparation of nanofibrous scaffold. It is demonstrated the aligned nanofibers provide a suitable condition for cell attachment and proliferation [68].

Also consistent with our result, previous study indicated the mechanical strength of aligned fibers were higher than randomly oriented ones [69].

The following four viewpoints summarize the underlying causes for these findings. First, using chitosan nanoparticles to fabricate the PLGA/CS composite enhances the hydrophilicity in both fabrication methods. Second, PLGA/CS nano-biocomposites fabricated by double nozzle method are very brittle and have not suitable mechanical properties for tissue engineering application. Third, the mechanical properties of the scaffolds fabricated by single nozzle method are improved by increasing the chitosan nanoparticles content. Fourth, a scaffold with a higher hydrophilicity and better mechanical properties has a higher PBS absorption, yielding more absorbed medium in the scaffold through cell culturing with a suitable mechanical support. Our findings indicate that the aligned nanofibrous scaffold with high percentage of chitosan nano-particles (3070Ad) provides a beneficial approach for tissue regeneration.

5. Conclusions

In this study, both the randomly oriented and the aligned PLGA and PLGA/CS nanofibrous scaffolds were fabricated using two different methods, namely, the single- and the double-nozzle methods. Scaffold composed of PLGA and chitosan nano-particles provide the mechanical support required and enhance the cell attachment and proliferation rate. In this study, chitosan nanoparticles and PLGA were used to fabricate the scaffolds by electrospinning method, for the first time. The resulting composites exhibited increased hydrophilicity of the composite scaffolds and improved mechanical properties by increasing chitosan content in the biocomposites scaffold in the first method. However, compared to the randomly oriented nanofibrous scaffolds, the aligned ones exhibited a higher tensile strength. These results demonstrate that the inherent hydrophobicity of synthetic PLGA can be modified by incorporating a suitable amount of chitosan. In addition, the fabricated biocomposites by the first method showed various synergic effects including enhanced PBS absorption and increased hydrophilicity. Thus aligned nanofibrous scaffold with high percentage of chitosan nanoparticles (3070 Ad) provide a beneficial approach for tissue engineering.

Acknowledgments

The authors are grateful to Isfahan University of Technology (IUT) for their support and Mrs. Aliakbari for kind collaboration.

Funding

The authors are grateful to Iranian Council of Stem Cell Technology, Isfahan University of Medical Sciences, for financial support (grant No. 190044).

References

- Kenawy, E. R.; Layman, J. M.; Watkins, J. R.; Bowlin, G. L.; Matthews, J. A.; Simpson, D. G. *Biomaterials* **2003**, *24*, 907.
- Li, W. J.; Laurencin, C. T.; Caterson, E. J.; Tuan, R. S.; Ko, F. K. *J. Biomed. Mater. Res.* **2002**, *60*, 613.
- Lu, Y. K.; Kim, K.; Hsiao, B. S.; Chu, B.; Hadjiafragyrou, M. *J. Control. Release* **2003**, *89*, 341.
- Matthews, J. A.; Wnek, G. E.; Simpson, D. G.; Bowlin, G. L. *Biomacromolecules* **2002**, *3*, 232.
- Yoshimoto, H.; Shin, Y. M.; Terai, H.; Vacanti, J. P. *Biomaterials* **2003**, *24*, 2077.
- Min, B. M.; You, Y.; Kim, J. M.; Lee, S. J.; Park, W. H. *Carbohydr. Polym.* **2004**, *57*, 285.
- Hutmacher, D. W.; Sittiger, M.; Risbud, M. V. *Trends Biotechnol.* **2004**, *22*, 354.
- Gomes, M. E.; Godinho, J. S.; Tchalamov, D.; Cunha, A. M.; Reis, R. L. *Mater. Sci. Eng. C* **2002**, *20*, 19.
- Mano, J. F.; Vaz, C. M.; Mendes, S. C.; Reis, R. L.; Cunha, A. M. *J. Mater. Sci. Mater. Med.* **1999**, *10*, 857.
- Sill, T. J.; von Recum, H. A. *Biomaterials* **2008**, *29*, 1989.
- Yoon, H.; Kim, G. *J. Biomater. Sci. Polym. Ed.* **2010**, *21*, 553.
- Smith, L. A.; Liu, X.; Ma, P. X. *Soft Matter* **2008**, *4*, 2144.
- Sridhar, R.; Sundarrajan, S.; Venugopal, J. R.; Ravichandran, R.; Ramakrishna, S. *J. Biomater. Sci. Polym.* **2013**, *4*, 24.
- Andukuri, A.; Kushwaha, M.; Tambralli, A.; Anderson, J. M.; Dean, D. R.; Berry, J. L. *Acta Biomater.* **2011**, *7*, 225.
- Li, X. K.; Cai, S. X.; Liu, B.; Xu, Z. L.; Dai, X. Z.; Ma, K. W.; Li, S. Q.; Yang, L.; Paul Sung, K. L.; Fu, X. B. *Colloids Surf., B* **2007**, *57*, 198.
- Liu, B.; Cai, S. X.; Ma, K. W.; Xu, Z. L.; Dai, X. Z.; Yang, L. *J. Mater. Sci. Mater. Med.* **2008**, *19*, 1127.
- Fan, X.; Guo, L.; Liu, T. *Polym.-Plast. Technol. Eng.* **2013**, *6*, 52.
- Hsu, S. H.; Seng Lu, P.; Ni, H. C.; Su, C. H. *Biomed. Microdev.* **2007**, *9*, 665.
- Evans, G. R. D.; Brandt, K.; Widmer, M. S.; Lu, L.; Meszlenyi, R. K.; Gupta, P. K. *Biomaterials* **2002**, *23*, 841.
- Evans, G. R. D.; Brandt, K.; Widmer, M. S.; Lu, L.; Meszlenyi, R. K.; Gupta, P. K. *Biomaterials* **1999**, *20*, 1109.
- Bian, Y. Z.; Wang, Y.; Aibaidoula, G.; Chen, G. Q.; Wu, Q. *Biomaterials* **2009**, *30*, 217.
- Yucel, D.; Torun Kose, G.; Hasirci, V. *Biomaterials* **2010**, *31*, 1596.
- Chen, Y. Sh.; Chang, J. Y.; Cheng, C. Y.; Tsai, F. J.; Yao, C. H.; Liu, B. S. *Biomaterials* **2005**, *26*, 3911.
- Meng, Z. X.; Wang, Y. S.; Ma, C.; Zheng, W.; Li, L.; Zheng, Y. F. *Mater. Sci. Eng. C* **2010**, *30*, 1204.
- Yao, L.; de Ruiter, G. C. W.; Wang, H.; Knight, A. M.; Spinner, R. J.; Yaszemski, M. J. *Biomaterials* **2010**, *31*, 5789.
- Yang, L.; Fitie, C. F. C.; Van der Werf, K. O.; Bennink, M. L.; Dijkstra, P. J. *Biomaterials* **2008**, *29*, 955.
- (a) Kumar, S.; Kumari, M.; Dutta, P. K.; Koh, J. *Int. J. Polym Mater. Polym. Biomater.* **2014**, *63*, 4; (b) Cheng, H.; Huang, Y. C.; Chang, P. T.; Huang, Y. Y. *Biochem. Biophys. Res. Commun.* **2007**, *357*, 938.

28. Ma, L.; Gao, C. Y.; Mao, Z. W.; Zhou, J.; Shen, J. C.; Hu, X. Q. *Biomaterials* **2003**, *24*, 4833.
29. Wu, L.; Ding, J. *Biomaterials* **2004**, *25*, 5821.
30. Athanasiou, K. A.; Niederauer, G. G.; Agrawal, C. M. *Biomaterials* **1996**, *17*, 93.
31. Wu, L.; Ding, J. *Biomaterials* **2004**, *25*, 5821, 25.
32. Li, X. K.; Cai, S. X.; Liu, B.; Xu, Z. L.; Dai, X. Z.; Ma, K. W. *Colloids Surf., B* **2007**, *57*, 198.
33. Glowacki, J.; Mizuno, S. *Biopolymers* **2008**, *89*, 338.
34. Drury, J. L.; Mooney, D. J. *Biomaterials* **2003**, *24*, 4337.
35. Yang, Y.; Zhu, X.; Cui, W.; Li, X.; Jin, Y. *Macromol. Mater. Eng.* **2009**, *294*, 611.
36. Zhao, H.; Ma, L.; Gao, C.; Shen, J. *J. Biomed. Mater. Res. Part B* **2009**, *88*, 240.
37. Khnor, E.; Lim, L. *Biomaterials* **2003**, *24*, 2339.
38. No, H. K.; Park, N. Y.; Lee, S. H.; Meyers, S. P. *Int. J. Food Microbiol.* **2002**, *74*, 65.
39. Ueno, H.; Mori, T.; Fujinaga, T. *Adv. Drug Delivery Rev.* **2001**, *52*, 105.
40. Ravi Kumar, M. N. V. *React. Funct. Polym.* **2000**, *46*, 1.
41. Bumgardner, J. D.; Wiser, R.; Gerard, P.; Bergin, P.; Chestnutt, B.; Marini, M. *J. Biomater. Sci. Polym. Ed.* **2003**, *14*, 423.
42. Cheng, M.; Gong, K.; Li, J.; Gong, Y.; Zhao, N.; Zhang, X. *J. Biomater. Appl.* **2004**, *19*, 59.
43. Shanmugasundaram, N.; Ravichandran, P.; Reddy, P. N.; Ramamurty, N.; Pal, S.; Rao, K. P. *Biomaterials* **2001**, *22*, 1943.
44. Kuo, Y. C.; Ku, I. N. *Biomacromolecules* **2008**, *9*, 2662.
45. Gong, H. P.; Zhong, Y. H.; Li, J. C.; Gong, Y. D.; Zhao, N. M.; Zhang, X. F. *J. Biomed. Mater. Res.* **2000**, *52*, 285.
46. Kuo, Y. C.; Yeh, C. F.; Yang, J. T. *Biomaterials* **2009**, *30*, 6604.
47. Min, B. M.; Lee, S. W.; Lim, J. N.; You, Y.; Lee, T. S.; Kang, P. H. *Polymer* **2004**, *45*, 7137.
48. Huang, X. J.; Ge, D.; Xu, Z. K. *Eur. Polym. J.* **2007**, *43*, 3710.
49. Kriegel, C.; Kit, K. M.; McClements, D. J.; Weiss, J. *Polymer* **2009**, *50*, 189.
50. Jung, K. H.; Huh, M. W.; Meng, W.; Yuan, J.; Hyun, S. H.; Bae, J. S. *J. Appl. Polym. Sci.* **2007**, *105*, 2816.
51. Peesan, M.; Rujiravanit, R.; Supaphol, P. *J. Biomater. Sci. Polym. Ed.* **2006**, *17*, 547.
52. Jayakumar, R.; Prabaharan, M.; Nair, S. V.; Tamura, H. *Biotechnol. Adv.* **2010**, *28*, 142.
53. Hong, S.; Kim, G. H. *Carbohydr. Polym.* **2011**, *38*, 940.
54. Vaezifar, S.; Razavi, S.; Golozar, M. A.; Karbasi, S.; Morshed, M.; Kamali, M. *J. Cluster Sci.* **2013**, *24*, 891.
55. Deitzel, J. M.; Kleinmeyer, J.; Harris, D.; Tan, N. C. B. *Polymer* **2001**, *42*, 261.
56. Cheng, M.; Deng, J.; Yang, F.; Gong, Y.; Zhao, N.; Zhang, X. *Biomaterials* **2003**, *24*, 2871.
57. Chen, Z. G.; Mo, X. M.; He, C. G.; Wang, H. S. *Carbohydr. Polym.* **2008**, *72*, 410.
58. Hollister, S. J. *Nat. Mater.* **2005**, *4*, 518.
59. Murphy, C. M.; Haugh, M. G.; O'Brien, F. J. *Biomaterials* **2010**, *31*, 461.
60. Jose, M. V.; Thomas, V.; Dean, D. R.; Nyairo, E. *Polymer* **2009**, *50*, 3778.
61. Wang, T.; Turhan, M.; Gunasekaran, S. *Polym. Int.* **2004**, *53*, 911.
62. Tangsathakun, C. *J. Biomater. Sci. Polym. Ed.* **2007**, *18*, 147.
63. Peniche-Covas, C.; Arguelles-Monal, W.; Roman, J. S. *Polym. Degrad. Stab.* **1993**, *39*, 21.
64. Thomas, V.; Jose, M. V.; Chowdhury, S.; Sullivan, F.; Dean, D. R.; Vohra, Y. K. *J. Biomater. Sci. Polym. Ed.* **2006**, *17*, 984.
65. Shin, Y. M.; Hohman, M. M.; Brenner, M. P.; Rutledge, G. C. *Polymer* **2001**, *42*, 9955.
66. Hohman, M. M.; Shin, M.; Rutledge, G.; Brenner, M. P. *Phys. Fluids* **2001**, *13*, 2221.
67. Li, Q.; Wei, Q. F.; Wu, N.; Cai, Y. B.; Gao, W. D. *J. Appl. Polym. Sci.* **2008**, *107*, 3535.
68. Cooper, A.; Bhattachari, N.; Kievit, F. M.; Rossol, M.; Zhang, M. *Phys. Chem. Chem. Phys.* **2011**, *13*, 7.
69. Volova, T.; Goncharov, D.; Sukovaty, A.; Shabanov, A.; Nikolaeva, E.; Shishatskaya, E. *J. Biomater. Sci. Polym. Ed.* **2013**.